MM4Drone: A Multi-Spectral Image and mmWave Radar Approach for Identifying Mosquito Breeding Grounds via Aerial Drones

K.T.Y. Mahima[1], Malith Weerasekara[1], Kasun De Zoysa[1], Chamath Keppitiyagama[1], Markus Flierl[2], Luca Mottola[3,4], and Thiemo Voigt[3,4]

[1] University of Colombo, School of Computing, Sri Lanka
[2] KTH Royal Institute of Technology, Electrical Engineering and Computer Science, Stockholm, Sweden
[3] RISE Research Institutes of Sweden, Sweden
[4] Uppsala University, Department of Information Technology, Sweden
{yasasm,malithk}@scorelab.org, {kasun,chamath}@ucsc.cmb.ac.lk, mflierl@kth.se, luca.mottola@ri.se, thiemo.voigt@it.uu.se

Abstract. Mosquitoes spread disases such as Dengue and Zika that affect a significant portion of the world population. One approach to hamper the spread of the disases is to identify the mosquitoes' breeding places. Recent studies use drones to detect breeding sites, due to their low cost and flexibility. In this paper, we investigate the applicability of drone-based multi-spectral imagery and mmWave radios to discover breeding habitats. Our approach is based on the detection of water bodies. We introduce our Faster R-CNN-MSWD, an extended version of the Faster R-CNN object detection network, which can be used to identify water retention areas in both urban and rural settings using multi-spectral images. We also show promising results for estimating extreme shallow water depth using drone-based multi-spectral images. Further, we present an approach to detect water with mmWave radios from drones. Finally, we emphasize the importance of fusing the data of the two sensors and outline future research directions.

Keywords: Multispectral Imagery · mmWave Radar · Aerial Drones · Object Detection.

1 Introduction

Dengue and Zika are two arboviral viruses that affect a significant portion of the world population. Each year, almost 400 million dengue infections happen. Due to severe dengue fever, around half a million people each year are in need of hospitalization [39] and about 36.000 people die [23]. The number of dengue cases varies from year to year. After a reduction in many countries of the world in 2017, the numbers are increasing again [39]. In Sri Lanka alone, the number of dengue cases has been substantial in recent years with more than 150.000 cases of dengue reported in 2017 [1] (see Fig. 1). In 2017, 440 people in Sri Lanka died of

dengue fever. According to government reports, the dengue patient management cost has reached 2 million USD in the year 2012 (when the number of cases was much lower than in 2017 and 2019) only for the Colombo district of Sri Lanka [24].

While there is no direct correlation between the income level of the people and the possibility of being infected by the dengue virus, the economic impact on the poor is much larger. According to Senanayake et al. [29] funds spent by households below the poverty-line for the treatment of dengue amounted to 93.7% of monthly per capita income. This is despite the fact that free health care is available in Sri Lanka.
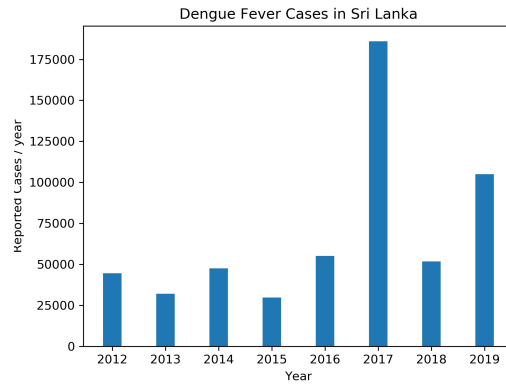

Fig. 1: Dengue Fever Cases in Sri Lanka. Some years more than 100000 cases with a strong health and economic impact, in particular on the poor part of the population.

Dengue spreads rapidly in densely populated urban areas. The principle vector species of both dengue and zika viruses are the mosquitoes Aedes aegypti and Aedes albopictus [8]. They breed in very slow-flowing or standing water pools. It is important to reduce and control such potential breeding grounds to contain the spread of these diseases. The roofs of buildings in urban environments, especially blocked gutters, provide ideal breeding grounds for Aedes. In Sri Lanka, there is a National Dengue Control Unit (see http://www.dengue.health.gov.lk/) to address this problem. Public health officials, police and military personnel visually inspect lands and buildings to locate potential mosquito breeding sites. This is difficult for the roofs of tall buildings despite that these may contain potential water collecting structures.

In this paper, we present our approach to fight dengue fever. In particular, we propose to use drones equipped with multi-spectral imagery cameras and mmWave radios to provide aerial inspection capabilities. This paper describes our system design and presents initial results in two of the projects' direction. First, we discuss how we use multi-spectral imagery to detect water from drone

flights. In particular, we present our experiments to detect water retention areas from deep learning based object detection utilizing drone-based multi-spectral images. To the best of our knowledge, this is the first work that introduces a water detection method via deep-learning-based object detection and multi-spectral imagery. Moreover, estimating water depth using the bathymetric log-ratio algorithm [33] with the drone-based multi-spectral images is also not assessed yet. In summary, the main contributions of this work are as follows: (a) Demonstrate the applicability of the mmWave radios to detect water. (b) Introduce a deep-learning-based object detection network to detect water bodies via multi-spectral images. (c) Use multi-spectral images recorded by a drone to illustrate how the bathymetric log-ratio approach can be used to assess water depth.

The remainder of this paper is organized as follows: The state-of-the-art methods for drone-based detection of water using mmWave radios and multi-spectral images are outlined in Section 2. Section 3 discusses the system that the authors intend to develop. Section 4 presents our approaches for multi-spectral images, the related experiments and results to detect water retention areas. Section 5 discusses our drone-based water detection method using mmWave radar. Finally, Section 6 summarises our findings and concludes the paper.

2   Related Work

Joshi and Miller review machine learning techniques for mosquito control [17]. Like us, they focus on urban environments due to the high number of cases of mosquito-borne diseases in such areas. They highlight the challenges and progress in the area of visual detection for identifying mosquitoes. Vasconcelos et al. present an IoT-based prototype for counting mosquitoes [37]. In particular, they detect and classify mosquitoes based on the sound of their wingbeats.

Texas Instruments have presented a demonstration on applying mmWave radios to classify water and ground in a lab environment [15]. Shui et al. recently presented a system for measuring water depth using mmWave radios as we do [30]. We are aiming at going one step beyond by trying to measure water depth from drones which causes additional challenges. Other related applications of mmWave radios include the 2D rotor orbit of rotating machinery [11] as well as robust indoor mapping even in harsh environments such as in smoke-filled conditions [18].

Drones are capable of reaching locations that humans are unable to easily reach and they enable rapid observation of the ground with low operation cost. In recent research, drones are being used extensively in mosquito breeding habitat observation and other control measures such as spraying larvicides [2–5, 7, 9, 27, 36, 38]. In particular, drone-based multi-spectral imagery has also been used in several studies to determine areas that are likely to be breeding grounds [32, 6, 22, 28]. These studies have focused on locating relatively large water bodies in rural and peri-urban areas, such as ponds, temporary water pools and road puddles. However, we are looking for water retention areas in all urban (e.g. water retention areas on rooftops), peri-urban and rural areas.

3   System Description

This section briefly describes the system that we are implementing. Our goal is to detect the breeding places, i.e., still-standing water with mosquito larvae, in densely populated areas using drones. The detection of the breeding places happens in two steps: first drones are sent on what we call scanning flights at high altitude (around 300 meters) to identify areas that need to be more closely investigated. The scanning flights will be based on digital maps that indicate potential breeding places, using open formats such as OpenStreetMap Keyhole Markup Language (KML) that facilitate the exchange of map information among involved stakeholders.

We construct the initial version of the maps with the help of public health instructors who currently do this job manually and hence have in-depth knowledge. We then automatically update the maps with data from new flights as well as weather information, for example, to include the effects of recent rainfalls that may create new potential breeding places. Based on the updated maps we construct the paths that consist of the waypoints, i.e., the potential breeding places for closer inspection flights.

In the second step, drones visit the waypoints. When arriving at a potential breeding place, the task of the drone is to detect and analyze the water area and determine whether or not it contains mosquito larvae. We investigate two approaches to solve this problem: First, we employ mmWave radios to detect water retention areas as potential mosquito habitats. Second, we use multi-spectral images to analyze the water area, measure the depth of the water and understand the larvae density. After that, we fuse the results for the final classification of the water area. Once we have detected a breeding place with mosquito larvae, the public health authorities and building owners are informed to ensure removal of the breeding place. Another option is to use spray larvicides or drop larvicide tablets into water with larvae.

4   Using Multi-spectral Imagery to Detect Mosquito Breeding Places

In this section, we discuss the usability of multi-spectral imagery to detect larval habitats. First, we discuss the drone-based multi-spectral image data that is available for processing. Then we focus on the detection of water as a potential breeding place. Here, the urban scenario is of particular interest. Finally, we emphasize the importance of water depth for larval habitats and its estimation from multi-spectral drone imagery.

4.1   Drone-based Multi-spectral Image Data

Previous research on mosquito breeding ground detection is based on identifying near standing water bodies or water retention areas using natural colour (RGB) aerial imagery [2–4, 27]. However, the information attainable from RGB images

is limited when compared to that of multi-spectral imagery. For example, multi-spectral images from drones have successfully been used in combination with machine learning (ML) techniques to detect larval habitats in rural areas more accurately [6]. Our focus is on urban areas and the use of deep learning (DL) techniques to detect actual larval habitats in a challenging urban environment. Therefore, we collect our data with a MicaSense RedEdge-MX multi-spectral camera fitted onto a DJI Phantom 4 drone as shown in Fig. 2. The sensor has five spectral bands: Blue, Green, Red, Red Edge, and Near-Infrared (NIR).

Fig. 2: MicaSense RedEdge-MX camera mounted on a DJI Phantom 4 drone.

4.2   Detecting Water Using Multi-spectral Imagery

Several studies have been done to identify water bodies using multi-spectral image datasets from satellites such as Landsat[1]. In recent years, drone-based multi-spectral images have been widely collected for different purposes. The applications range from agricultural data analysis to the detection of water areas. For this purpose, different methods have been developed.

Multi-spectral Indices
    The basic methods utilize multi-spectral indices to detect water areas. We have assessed the applicability of the Normalized Difference Water Index (NDWI) [21] to classify pixels as water or non-water pixels. We have determined the index from the source images available for the spectral bands of the MicaSense RedEdge-MX sensor. The NDWI is defined as

$$\mathrm{NDWI} = \frac{\mathrm{Green} - \mathrm{NIR}}{\mathrm{Green} + \mathrm{NIR}}. \tag{1}$$

The index ranges from -1 to 1. Values above zero indicate water features. Values below or equal to zero suggest non-water features such as soil and vegetation [21].

---

[1] https://landsat.gsfc.nasa.gov/data/

An experiment in an environment with water on concrete ground is instructive. We learn that the NDWI is not able to properly segment the concrete area retaining water. Further, the definition of the NDWI in Eq. 1 indicates that it is highly correlated with plant water content by using NIR and Green bands [21]. Hence, using only the NDWI for identifying potential mosquito breeding places in urban environments such as water retention areas on rooftops is challenging. Therefore, more advanced methods like ML techniques have to be used for multi-spectral imagery to identify potential mosquito breeding places in urban areas.

Deep-learning-based Methods for Detection of Water Areas

Minakshi et al. [22] recently demonstrated the suitability of CNN-based object detection for aerial imagery by experimenting with an Inception V2 [35] network for feature extraction and a Faster Region-based CNN (Faster R-CNN) [25] with a bounding box based method to localize the areas of larval habitats. Since our primary goal is to identify potential breeding habitats in urban environments, such an object detection approach appears appealing. Here, the open question is the adequate size of the utilized bounding box. In urban environments, the diversity of water retention areas is high. Segmentation methods may become more challenging and bounding box-based detection may become more efficient and reliable.

In this study, we extend the CNN-based object detection approach proposed by Minakshi et al. [22] to process multispectral images. In order to handle 5-band multi-spectral stacked images, we modify the initial Keras Faster R-CNN network[1] as well as the pre-processing workflow. For feature extraction, we utilize either ResNet-50 [12] or VGG [31] networks. Fig. 3 depicts the proposed Faster R-CNN training pipeline with the stacked multi-spectral image. We refer to it as the Faster R-CNN Multi-Spectral Water Detection (Faster R-CNN-MSWD) network.
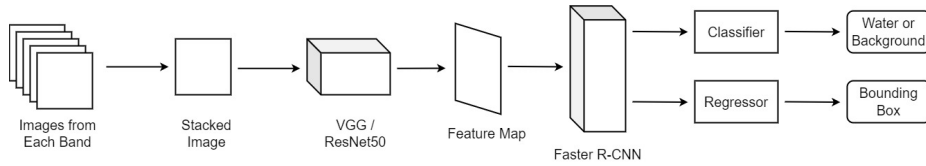

Fig. 3: Faster R-CNN model for multi-spectral images. First, the images from each band are combined into a single stacked image. A VGG or ResNet50 network is used to extract feature maps. These feature maps are then used by the Faster R-CNN to localize water areas.

For the experiments, we gather a multi-spectral image dataset using our camera and drone. First, we create the stacked image of 5 bands and the corresponding RGB images for all images in our dataset. Then, we use the RGB images to

---

[1] https://github.com/you359/Keras-FasterRCNN

annotate manually the water retention regions via rectangular bounding boxes. As the size of RGB and stacked images match, we can use the bounding boxes to train the network with the stacked images. Currently, our dataset includes 112 stacked images that depict water retention areas. Finally, we use 70% of the stacked images for training and 30% for testing our Faster R-CNN-MSWD network.
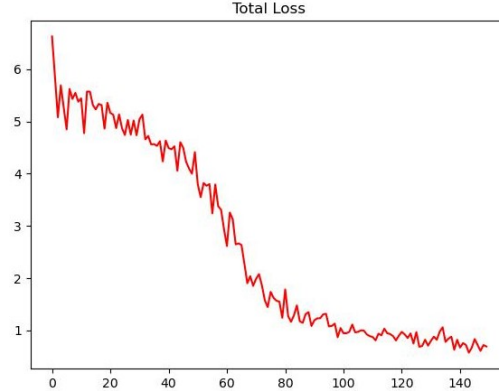

Fig. 4: Total loss of our Faster R-CNN-MSWD network with a VGG backbone. The x-axis gives the number of epochs. The y-axis shows the loss value.

We train our Faster R-CNN-MSWD with a VGG region proposal network (RPN). With this VGG backbone network, we have 136,699,171 trainable parameters. In the training phase, we reduce the total training loss to 0.575. For our test data, we achieve a mean average precision (mAP) of 0.89 at an IoU of 0.25 (Intersection over Union). However, due to the lack of training samples, we observe a relatively high number of false negatives (FN), i.e, not detected bounding boxes. The training loss curve of our Faster R-CNN-MSWD with a VGG backbone is shown in Fig. 4. Loss values for RPN and detector networks are summarized in Table 1.

Table 1: Loss values of RPN and detector networks of the Faster R-CNN-MSWD with a VGG.

RPN Classification Loss	RPN Regression Loss	Detector Classification Loss	Detector Regression Loss
0.379	0.079	0.061	0.054

Faster R-CNN-MSWD and VGG are trained using an Intel(R) Core(TM) i7-8700K CPU, an NVIDIA GTX 1080 Ti GPU and 32GB RAM. To visualize the detection results for a multi-spectral stacked image, we add the predicted bounding boxes to the corresponding RGB image, as shown in Fig. 5.

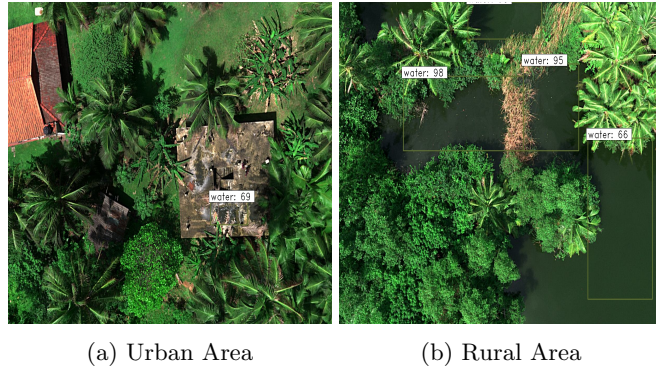(a) Urban Area   (b) Rural Area

Fig. 5: Water retention areas as detected by the Faster R-CNN-MSWD with VGG. The bounding boxes are added to the corresponding RGB image of the given stacked multi-spectral image. Our network is able to detect water retention areas in both urban (including rooftops as shown in Fig. 5a) and rural (including large water bodies as shown in Fig. 5b) areas.

4.3   Water Depth Estimation Using Multi-spectral Imagery

The depth of water has been identified as a vital factor that influences mosquito larval development [32, 26, 34]. Several studies have been conducted in order to determine water depth using multi-spectral satellite imagery [33, 19, 10]. Recently, Sarira et al. conducted a study to determine the minimum water depth such that water areas can be accurately identified by multi-spectral images [28]. As a result, they found that there is a considerable statistical dependency between NIR reflectance and water depth. In particular, they show that it requires at least 5-10 cm depth for an accurate identification of inundated areas using NIR images.

Motivated by this, we have collected a dedicated image dataset of water buckets with varying water depths, ranging from 2-16 cm in increments of 1 cm. Our earlier paper [20] discusses our initial approach of using bathymetric models and band reflectances to estimate water depth from drone-based multi-spectral images. The log-ratio algorithm [33] in Eq. 2 has initially been introduced for satellite imagery to analyze shallow water of up to 15 m. We apply this model, determine the logarithm of the reflectance of the NIR band $R(NIR)$ and normalize it by the logarithm of the reflectance of the Blue band $R(Blue)$. The model assumes a linear relation between the depth and the log-ratio.

$$Z = m\frac{\log R(\lambda_i)}{\log R(\lambda_j)} + c \tag{2}$$

Here, Z denotes the water depth. $R(\lambda_i)$ and $R(\lambda_j)$ are the reflectance values of the NIR and Blue bands, respectively. m and c are the model parameters that can be determined by linear regression.

Fig. 6 depicts the regression plot of the initial experiment. The moderate variance of the data points around the linear regression line demonstrates the
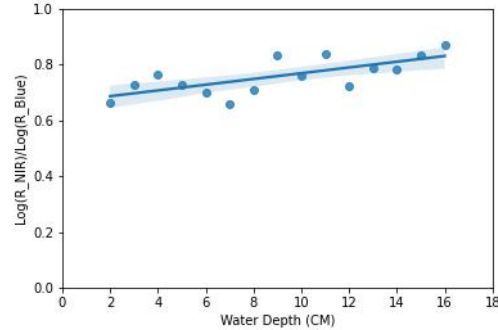
Fig. 6: Regression plot of water depth vs. log-ratio of the NIR and Blue band reflectance values. There is a linear relationship between $\log R(NIR) / \log R(Blue)$ and water depth. This indicates that we can use the bathymetric log-ratio method to estimate the water depth from drone-based multi-spectral images.

applicability of the bathymetric log-ratio algorithm to determine the depth of extremely shallow water areas using multi-spectral drone images. Note that some data points are rather noisy. In the future, we plan to improve the quality of the data in order to measure the depth of extremely shallow water areas more accurately.

The depth of water areas is just one feature to detect larval breeding grounds more reliably. Deep-learning-based approaches are promising when identifying potential mosquito habitats in urban areas. Spectral indices and water depth will be valuable features for such learning-based methods. However, a large volume of annotated images is necessary for well-performing deep-learning networks. In the future, we will collect an annotated urban image dataset that will allow us to train a feature-based network for reliable detection of larval breeding grounds.

5 Using mmWave Radios to Detect Mosquito Breeding Places

In this section, we discuss the usability of mmWave radios to detect water areas. We start with a brief introduction of the mmWave radio technology. Then we report on our experimental setup, preliminary results gained from the experiments and identified challenges.

5.1 MmWave Radio Technology

A mmWave radio transmits an electromagnetic signal (a chirp) using its transmission (TX) antennas and captures the reflection of the chirp by its receiving (RX) antennas [16]. Then the mmWave radio passes the RX signal and TX signal to the mixer and an intermediate frequency (IF) signal is the output that contains the frequency difference between the TX and RX signals (Fig. 7a). This

generated signal contains a single constant frequency and this frequency is proportional to the distance between the target from the mmWave sensor. When receiving RX signals from multiple objects with different distances, the resulting signal will be generated as a combination of multiple IF signals (Fig. 7b). By performing a Fast Fourier transform (FFT) one can compute the frequencies contained in the IF signal (Fig. 7c). The detected frequencies are then used to calculate the distance to the target and the receiving power of the signal [16].
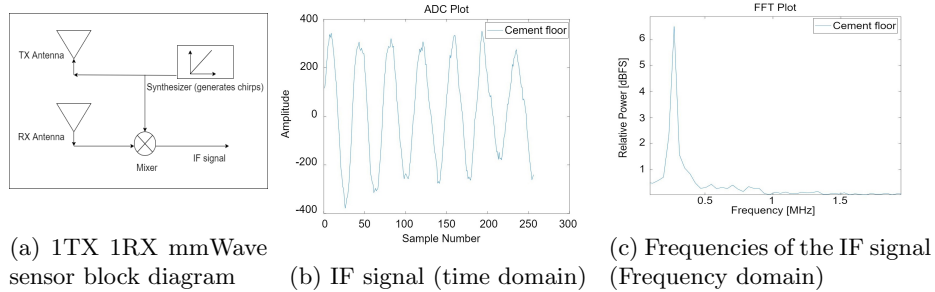

(a) 1TX 1RX mmWave sensor block diagram   (b) IF signal (time domain)   (c) Frequencies of the IF signal (Frequency domain)

Fig. 7: mmWave Sensing

5.2   Detecting Water Using mmWave Radios

For the experiments, we use a Texas Instrument IWR1843boost mmWave sensor and Texas instrument DCA1000 evaluation module for raw data capturing (see Fig. 8a). In particular, we conduct several lab experiments to uniquely differentiate water from other target materials like soil, wood, glass pallet, copper sheet and cardboard that were placed under the sensor at a distance of 1.5 m (see Fig. 8b).

(a) IWR1843boost mmWave sensor with DCA1000evm data capture card.   (b) Water detection setup in a Lab environment.   (c) mmWave sensor mounted on a DJI Phantom 4 Standard drone.

Fig. 8: Experimental setup for the mmWave sensor.

After obtaining the IF signals for each of these materials, we apply an FFT to get the corresponding frequencies and receiving power of the IF signal. Fig. 9

shows that we obtain different power levels for different materials. This follows from Eq. 3 [13].

$$\text{Power Captured at RX Antenna} = \frac{P_t G_{TX} A_{RX} \sigma}{(4\pi)^3 d^4} \qquad (3)$$

In this equation, P_t is the transmitted power, G_{TX} the TX antenna gain, A_{RX} the effective aperture area of the RX antenna, σ the radar cross-section (RCS) of the target and d is the distance.

According to Eq. 3, if we keep the target at a fixed distance of 1.5 m and the other variables are constant, the receiving power of the signal depends only on the target's RCS value. In general, the target's RCS value depends on its size, reflectivity of its surface, and its shape [14]. As a result, we receive different power levels for different materials. Hence, it is possible to only use the distance and receiving power when detecting water via mmWave radios.
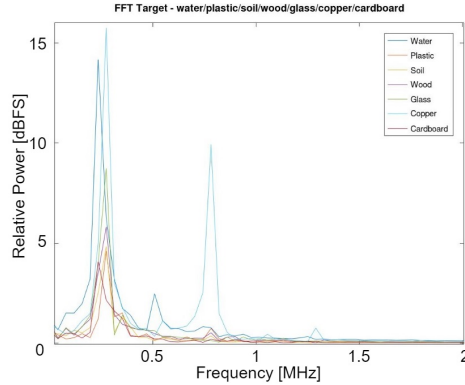

Fig. 9: Power levels of the mmWave radios for different materials. The receiving power is the highest for water but close to that of copper.

Fig. 9 shows that the IF signal's receiving power for water areas is relatively high compared to other materials assessed except copper. This implies that mmWave radios are able to detect water areas. However, it also confirms that we cannot rely solely on the mmWave sensor as some materials such as copper lead to similar receiving power levels. Therefore, to identify water with very high accuracy using a second technology such as imagery is required.

5.3   Detecting Water with mmWave Radios from Drones

We integrate the IWR1843boost mmWave sensor to the DJI Phantom 4 Standard drone as depicted in Fig. 8c. Notably, the TI IWR1843boost mmWave sensor is capable of working alone without connecting to the DCA1000 evaluation module and it has its own Digital Signal Processing (DSP) chip on it. To

record data from the mmWave sensor, we develop a python program[1] and run it on a Raspberry Pi Zero W module. Initially, we record two data sets targeting ground and water by hovering the drone at the same height. As depicted in the Fig. 10, the receiving power of the water areas are relatively high compared to the ground areas. This suggests that the mmWave radios can detect water from drones. The vibration of the drone generates instability in the receiving power of the signal. Hence, we use the average values for a window to stable the signal.
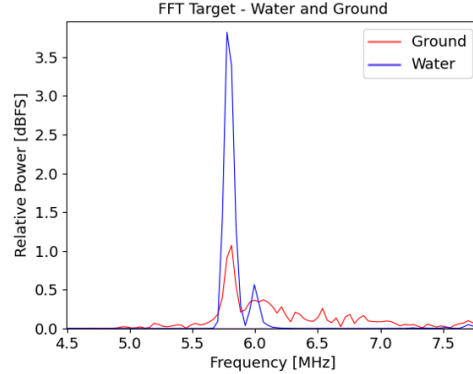

Fig. 10: Receiving Power for the ground and water

Based on the results we believe that further research on utilizing mmWave radios for detecting water using drones is essential. Moreover, we expect to verify that using mmWave radios to estimate water depth [30] is possible also from drones. Our results also indicate that fusing the results from mmWave radio and multi-spectral imagery would make the results more reliable.

6   Conclusions and Future Work

In this paper, we have evaluated multi-spectral imagery and mmWave radio waves to identify possible mosquito breeding areas by detecting water bodies. In particular, we propose our Faster R-CNN-MSWD network that uses drone-based multi-spectral images to detect both urban and rural water retention areas. Moreover, our results show that shallow water depth can be estimated from drone-based multi-spectral images by using a bathymetric method. Our experimental results further demonstrate that drone-based mmWave radios are capable of differentiating water areas from other targeted materials. In future work, we will collect more data and improve the Faster R-CNN-MSWD network.

It is unlikely that only one method will be able to accurately identify potential mosquito breeding sites. Hence, the fusion of multi-spectral and mmWave sensor data may lead to more reliable results. A system which incorporates both

---

[1] https://github.com/amweerasekara/mmWave-IWR1843Boost-UART-Data-Recorder

approaches may be used for a future commercial drone system that is able to detect breeding sites and automatically spray larvicides or drop larvicide tablets into the detected water bodies.

References

1. National dengue control unit, sri lanka. https://www.epid.gov.lk/web/index.php
2. Amarasinghe, A., Suduwella, C., Niroshan, L., Elvitigala, C., De Zoysa, K., Keppetiyagama, C.: Suppressing dengue via a drone system. In: 2017 Seventeenth International Conference on Advances in ICT for Emerging Regions (ICTer). pp. 1–7. IEEE (2017)
3. Amarasinghe, A., Wijesuriya, V.B.: Drones vs dengue: A drone-based mosquito control system for preventing dengue. In: 2020 RIVF International Conference on Computing and Communication Technologies (RIVF). pp. 1–6. IEEE (2020)
4. Andrade, G., Dias, T., Alves, V., Junior, H.A., Pinheiro, L., Pontes, R., Silva, B., de Macedo, I., Araujo, G., Prego, T., et al.: Fighting back zika, chikungunya and dengue: Detection of mosquito-breeding habitats using an unmanned aerial vehicle. IEEE CAS Student Design Competition **2018** (2017)
5. Bravo, D.T., Lima, G.A., Alves, W.A.L., Colombo, V.P., Djogbénou, L., Pamboukian, S.V.D., Quaresma, C.C., de Araujo, S.A.: Automatic detection of potential mosquito breeding sites from aerial images acquired by unmanned aerial vehicles. Computers, Environment and Urban Systems **90**, 101692 (2021). https://doi.org/https://doi.org/10.1016/j.compenvurbsys.2021.101692, https://www.sciencedirect.com/science/article/pii/S0198971521000995
6. Carrasco-Escobar, G., Manrique, E., Ruiz-Cabrejos, J., Saavedra, M., Alava, F., Bickersmith, S., Prussing, C., Vinetz, J.M., Conn, J.E., Moreno, M., et al.: High-accuracy detection of malaria vector larval habitats using drone-based multispectral imagery. PLoS neglected tropical diseases **13**(1), e0007105 (2019)
7. Case, E., Shragai, T., Harrington, L., Ren, Y., Morreale, S., Erickson, D.: Evaluation of Unmanned Aerial Vehicles and Neural Networks for Integrated Mosquito Management of Aedes albopictus (Diptera: Culicidae). Journal of Medical Entomology **57**(5), 1588–1595 (05 2020). https://doi.org/10.1093/jme/tjaa078, https://doi.org/10.1093/jme/tjaa078
8. Centers for Disease Control and Prevention: Surveillance and control of aedes aegypti and aedes albopictus in the united states. http://www.cdc.gov/chikungunya/resources/vector-control.html, accessed: 2016-04-11
9. Faraji, A., Haas-Stapleton, E., Sorensen, B., Scholl, M., Goodman, G., Buettner, J., Schon, S., Lefkow, N., Lewis, C., Fritz, B., Hoffman, C., Williams, G.: Toys or Tools? Utilization of Unmanned Aerial Systems in Mosquito and Vector Control Programs. Journal of Economic Entomology **114**(5), 1896–1909 (06 2021). https://doi.org/10.1093/jee/toab107, https://doi.org/10.1093/jee/toab107
10. Geyman, E.C., Maloof, A.C.: A simple method for extracting water depth from multispectral satellite imagery in regions of variable bottom type. Earth and Space Science **6**(3), 527—-537 (2019). https://doi.org/10.1029/2018EA000539
11. Guo, J., Jin, M., He, Y., Wang, W., Liu, Y.: Dancing waltz with ghosts: Measuring sub-mm-level 2d rotor orbit with a single mmwave radar. In: Proceedings of the

20th International Conference on Information Processing in Sensor Networks (co-located with CPS-IoT Week 2021). pp. 77–92 (2021)

12. He, K., Zhang, X., Ren, S., Sun, J.: Deep residual learning for image recognition. In: Proceedings of the IEEE conference on computer vision and pattern recognition. pp. 770–778 (2016)

13. Henriksen, S.: Radar-range equation. Proceedings of the IEEE **63**(5), 813–814 (1975). https://doi.org/10.1109/PROC.1975.9829

14. Hess, D.W.: Introduction to rcs measurements. In: 2008 Loughborough Antennas and Propagation Conference. pp. 37–44 (2008). https://doi.org/10.1109/LAPC.2008.4516860

15. Instruments, T.: (May 2017), https://training.ti.com/mmwave-water-vs-ground-classification-lab

16. Iovescu, C., Rao, S.: The fundamentals of millimeter wave sensors. Texas Instruments pp. 1–8 (2017)

17. Joshi, A., Miller, C.: Review of machine learning techniques for mosquito control in urban environments. Ecological Informatics **61**, 101241 (2021)

18. Lu, C.X., Rosa, S., Zhao, P., Wang, B., Chen, C., Stankovic, J.A., Trigoni, N., Markham, A.: See through smoke: robust indoor mapping with low-cost mmwave radar. In: Proceedings of the 18th International Conference on Mobile Systems, Applications, and Services. pp. 14–27 (2020)

19. Lyzenga, D.R., Malinas, N.P., Tanis, F.J.: Multispectral bathymetry using a simple physically based algorithm. IEEE Transactions on Geoscience and Remote Sensing **44**(8), 2251–2259 (2006). https://doi.org/10.1109/TGRS.2006.872909

20. Mahima, K.T.Y., Weerasekara, M., De Zoysa, K., Keppitiyagama, C., Mottola, L., Voigt, T., Flierl, M.: Fighting dengue fever with aerial drones. In: International Conference on Embedded Wireless Systems and Networks (EWSN) (2022)

21. McFeeters, S.K.: The use of the normalized difference water index (ndwi) in the delineation of open water features. International Journal of Remote Sensing **17** (1996). https://doi.org/10.1080/01431169608948714

22. Minakshi, M., Bhuiyan, T., Kariev, S., Kaddumukasa, M., Loum, D., Stanley, N.B., Chellappan, S., Habomugisha, P., Oguttu, D.W., Jacob, B.G.: High-accuracy detection of malaria mosquito habitats using drone-based multispectral imagery and artificial intelligence (ai) algorithms in an agro-village peri-urban pastureland intervention site (akonyibedo) in unyama sub–county, gulu district, northern uganda. Journal of Public Health and Epidemiology **12**(3), 202–217 (2020). https://doi.org/10.5897/JPHE2020.1213

23. Mosquito Reviews: Statistics for mosquito-borne diseases deaths. https://www.worldmosquitoprogram.org/en/learn/mosquito-borne-diseases/dengue (2022), https://www.worldmosquitoprogram.org, accessed: 2022-05-20

24. Neil Thalagal: Health system cost for dengue control and management in colombo district, sri lanka. Dengue Tool Surveilance Project, Epidemiology Unit Ministry of Health (2013)

25. Ren, S., He, K., Girshick, R., Sun, J.: Faster r-cnn: Towards real-time object detection with region proposal networks. IEEE Transactions on Pattern Analysis and Machine Intelligence **39**(6), 1137–1149 (2017). https://doi.org/10.1109/TPAMI.2016.2577031

26. Rohani, A., Najdah, W.M.A.W., Zamree, I., Azahari, A.H., Noor, I.M., Rahimi, H., Lee, H.L.: Habitat characterization and mapping of anopheles maculatus (theobald) mosquito larvae in malaria endemic areas in kuala lipis, pahang,

malaysia. The Southeast Asian journal of tropical medicine and public health **41 4**, 821–30 (2010)

27. Rossi, L., Backes, A., Souza, J.: Rain gutter detection in aerial images for aedes aegypti mosquito prevention. In: Anais do XVI Workshop de Visão Computacional. pp. 1–5. SBC (2020). https://doi.org/10.5753/WVC.2020.13474

28. Sarira, T.V., Clarke, K.D., Weinstein, P., Koh, L.P., Lewis, M.M.: Rapid identification of shallow inundation for mosquito disease mitigation using drone-derived multispectral imagery. Geospatial health **15 1** (2020). https://doi.org/10.4081/gh.2020.851

29. Senanayake, M., SK Jayasinghe, S., S Wijesundera, D., Manamperi, M.: Economic cost of hospitalized non-fatal paediatric dengue at the lady ridgeway hospital for children in sri lanka **43** (12 2014)

30. Shui, H., Geng, H., Li, Q., Du, L., Du, Y.: A low-power high-accuracy urban waterlogging depth sensor based on millimeter-wave fmcw radar. Sensors **22**(3), 1236 (2022)

31. Simonyan, K., Zisserman, A.: Very deep convolutional networks for large-scale image recognition. arXiv preprint arXiv:1409.1556 (2014)

32. Stanton, M.C., Kalonde, P., Zembere, K., Spaans, R.H., Jones, C.M.: The application of drones for mosquito larval habitat identification in rural environments: a practical approach for malaria control? Malaria journal **20**(1), 1–17 (2021). https://doi.org/https://doi.org/10.1186/s12936-021-03759-2

33. Stumpf, R.P., Holderied, K., Sinclair, M.: Determination of water depth with high-resolution satellite imagery over variable bottom types. Limnology and Oceanography **48**(1part2), 547–556. https://doi.org/10.4319/lo.2003.48.1_part_2.0547

34. Sutherland, A.: Mosquito management for ponds, fountains, and water gardens. UC IPM Retail Nursery amp; Garden Center IPM News **3 2** (Jun 2014), https://ucanr.edu/blogs/blogcore/postdetail.cfm?postnum=14396

35. Szegedy, C., Vanhoucke, V., Ioffe, S., Shlens, J., Wojna, Z.: Rethinking the inception architecture for computer vision. In: 2016 IEEE Conference on Computer Vision and Pattern Recognition (CVPR). pp. 2818–2826 (2016). https://doi.org/10.1109/CVPR.2016.308

36. Valdez-Delgado, K.M., Moo-Llanes, D.A., Danis-Lozano, R., Cisneros-Vázquez, L.A., Flores-Suarez, A.E., Ponce-García, G., Medina-De la Garza, C.E., Díaz-González, E.E., Fernández-Salas, I.: Field effectiveness of drones to identify potential aedes aegypti breeding sites in household environments from tapachula, a dengue-endemic city in southern mexico. Insects **12**(8) (2021). https://doi.org/10.3390/insects12080663, https://www.mdpi.com/2075-4450/12/8/663

37. Vasconcelos, D., Yin, M.S., Wetjen, F., Herbst, A., Ziemer, T., Förster, A., Barkowsky, T., Nunes, N., Haddawy, P.: Counting mosquitoes in the wild: An internet of things approach. In: Proceedings of the Conference on Information Technology for Social Good. pp. 43–48 (2021)

38. Williams, G.M., Wang, Y., Suman, D.S., Unlu, I., Gaugler, R.: The development of autonomous unmanned aircraft systems for mosquito control. PLOS ONE **15**(9), 1–16 (09 2020). https://doi.org/10.1371/journal.pone.0235548, https://doi.org/10.1371/journal.pone.0235548

39. World Mosquito Program: Statistics for mosquito-borne diseases deaths. https://mosquitoreviews.com/learn/disease-death-statistics (2022), https://mosquitoreviews.com/learn/disease-death-statistics, accessed: 2022-05-20